

Genome-wide transcriptomic analysis reveals the gene regulatory network that controlled by SRL1 in regulating rice leaf rolling

Xizhi Li

GuangXi University

Min Li

Guangxi University

Beibei Zhou

Guangxi University

Jinlin Bao

Guangxi University

Liang Zhu

GuangXi University

Pengbo Xue

Guangxi University

Jun Wang

Guangxi University

Jian Jin (✉ jinjian@gxu.edu.cn)

Guangxi University <https://orcid.org/0000-0002-1978-500X>

Original article

Keywords: SRL1/CLD1, rolling leaf, RNA-seq, bulliform cells, cuticle

Posted Date: February 7th, 2020

DOI: <https://doi.org/10.21203/rs.2.22853/v1>

License: © ⓘ This work is licensed under a Creative Commons Attribution 4.0 International License.

[Read Full License](#)

1 **Genome-wide transcriptomic analysis reveals the gene regulatory network that controlled by**

2 ***SRL1* in regulating rice leaf rolling**

3

4

5

6 Xizhi Li[#], Min Li[#], Beibei Zhou, Jinlin Bao, Liang Zhu, Pengbo Xue, Jun Wang^{*} and Jian Jin^{*}

7

8

9 State Key Laboratory for Conservation and Utilization of Subtropical Agro-bioresources, College

10 of Life Science and Technology, Guangxi University, Nanning 530005, China

11 [#] These authors contributed equally to this work

12 Author for correspondence:

13 Jun Wang (Email: wangjun.555-123@163.com) and Jian Jin (Email: jinjian@gxu.edu.cn)

14

15

16

17

18 **Abstract**

19 **Background**

20 *SRL1* (*SEMI-ROLLED LEAF 1*) also named as *CLD1* (*CURLED LEAF AND DWARF 1*),
21 encoding a putative glyphospholipidininol-anchored membrane protein, has been characterized as a
22 gene involved in the regulation of leaf morphology in rice. Mutants of *srll-1* (point mutation) and
23 *srll-2* (transferred DNA insertion) exhibit defects in leaf development resulting in a phenotype
24 with adaxially rolled leaves.

25 **Results**

26 To explore the gene regulatory network of leaf development that controlled by *SRL1* in rice, we
27 created a homozygous *SRL1* knock out (KO) line by CRISPR/Cas9, which showed defects in leaf
28 development with adaxially rolling. By comparing the leaf transcriptome of a homozygous *SRL1*
29 KO line (*srll-KO*) with the control, a total number of 3,178 genes were identified as differentially
30 expressed genes, of which 1,216 genes were significantly up regulated, while 1,962 genes were
31 down regulated. Further analyses indicated that, a group of known leaf rolling related genes,
32 which involved in bulliform cells and cuticle development such as *OsZHD1*, *OsLBD3-7*, *RFS*,
33 *ACL1*, *CFL1*, *SND1*, *OsCESA5* and *OsCESA6* were up or down regulated in the *srll-KO*.

34 **Conclusions**

35 *SRL1* might control leaf rolling by regulating a couple of genes that affecting cytological
36 architecture of leaf cells such as bulliforms and cuticle of leaves.

37 **Keywords:** *SRL1/CLD1*, rolling leaf, RNA-seq, bulliform cells, cuticle

38 **Background**

39 Rice is one of the most widely cultivated crops feeding more than half of the population around
40 the globe. As the major photosynthetic organ of plants, the photosynthetic efficiency of leaves has
41 a great influence on rice yield (Walter et al 2009). Therefore, it is of great significance to study the
42 mechanism of leaf development to improve rice yield. In recent years, many genes involved in
43 leaf development have been identified (Xu et al 2018).

44 *SRL1* (*SEMI-ROLLED LEAF 1*), which encodes a putative glycosylphosphatidylinositol
45 (GPI)-anchored protein (GAP) has been cloned and characterized as a gene that involves in
46 modulating leaf rolling. *SRL1* is expressed in various tissues and SRL1 protein is located
47 predominantly at the plasma membrane. Both of *srl1-1* (point mutant) and *srl1-2* (transferred
48 DNA insertion, knockdown mutant) displayed adaxially rolled leaves due to the increase of
49 bulliform cells at the adaxial cell layer. Laser microdissection and microarray analysis with the
50 cells that will become epidermal cells in wild type but bulliform cells in *srl1-1* indicated that the
51 genes encoding vacuolar H⁺-pyrophosphatase and H⁺-ATPase were up regulated in *srl1-1*,
52 suggesting that *SRL1* regulates leaf rolling through inhibiting the formation of bulliform cells by
53 repressing the expression of the genes encoding vacuolar H⁺-pyrophosphatase and H⁺-ATPase
54 (Xiang et al 2012). *CLD1* (*CURLED LEAF AND DWARF 1*) is allelic with *SRL1*. In addition to
55 adaxially rolled leaves, the *cldl* mutant, which was controlled epigenetically through DNA
56 methylation at the *SRL1* locus showed multiple morphological abnormalities, including the twisted
57 rolling leaves, dark-green leaves, dwarf of plant architecture, and faster water loss. The

58 quantitative proteomic analysis showed that a group of proteins, which associated with cell wall
59 formation, epidermis development and water stress, were differentially expressed between the
60 *cld1* mutant and the wild type (Li et al 2017).

61 In addition to *SRL1/CLD1*, a group of genes that regulate leaf rolling by affecting number and/or
62 area of bulliform cells have been cloned and functional characterized, including *YAB1 (YABBY1)*,
63 *OsZHD1 (ZINC FINGER HOMEODOMAIN 1)*, *OsZHD2*, *LC2 (LEAF INCLINATION 2)*, *RFS*
64 (*ROLLED FINE STRIPED*), *RL14 (ROLLING LEAF 14)*, *NRL1 (NARROW AND ROLLED LEAF*
65 *1)*, *OsMYB103L*, *ROC5 (RICE OUTER CELL SPECIFIC 5)*, *PFL (PROTODERMAL FACTOR*
66 *LIKE 1)*, *ACL1 (ABAXIALLY CURLED LEAF 1)*, *ACL2*, *REL1 (ROLLED AND ERECT LEAF 1)*,
67 *REL2*, *OsLBD3-7 (LATERAL ORGAN BOUNDARIES DOMAIN 3-7)*, *NAL7 (NARROW LEAF 7)*,
68 *NAL2/3*, *OsI-BAK1 (BRASSINOSTEROID INSENSITIVE 1-ASSOCIATED KINASE 1)*, *OsARF18*
69 (*AUXIN RESPONSE FACTOR 18*), *SLL2 (SHALLOT-LIKE 2)* and *OsRRK1 (RECEPTOR-LIKE*
70 *CYTOPLASMIC KINASE 1)* (Chen et al 2015, Cho et al 2018, Cho & Paek 2016, Dai et al 2007,
71 Fang et al 2012, Fujino et al 2008, Hu et al 2010, Huang et al 2016, Khew et al 2015, Li et al 2016,
72 Li et al 2010, Ma et al 2017, Xu et al 2014, Yang et al 2014, Yang et al 2016, Zhang et al 2015,
73 Zhao et al 2010, Zou et al 2011). Moreover, genes involved in regulation of leaf polarity such as
74 *ADL1 (ADAXIALIZED LEAF 1)*, *SLL1 (SHALLOT-LIKE 1)* and *OsAGO7 (ARGONATUE 7)*
75 (Hibara et al 2009, Shi et al 2007, Zhang et al 2009); genes related to development of
76 sclerenchymatous cells such as *NRL2/SRL2*, *SLL1* and *RL14* (Liu et al 2016, Zhang et al 2009,
77 Zhao et al 2016); genes related to cuticle development such as *CFL1 (CURLY FLAG LEAF 1)* and
78 *OsMYB103L* (Wu et al 2011, Yang et al 2014); miRNAs (miR160 and miR166) with their targets
79 (*OsARF18* and *OsHB4 (HOMEODOMAIN CONTAINING PROTEIN 4)*) and the genes involved

80 in processing miRNA (*DCL1* (*DICER-LIKE 1*), *OsAGO1*, *OsAGO7*) also have been proved to
81 regulate leaf rolling (Huang et al 2016, Liu et al 2005, Shi et al 2007, Wu et al 2009).

82 The gene regulatory network controlling by *SRL1/CLD1* have been studied previously using
83 transcriptomic analysis (microarray) with *srl1-1* and the iTRAQ (isobaric tags for the relative and
84 absolute quantitation) base proteomic analysis with *clld1*. However, the previous transcripomic
85 study focused on the genes expression difference in a group of cells that abutting the midrib at the
86 adaxial surface of leaf blades which would become epidermal cells in wild type and probably
87 bulliform cells in the *SRL1* point mutant *srl1-1*, this may lead to a incomplete understanding of the
88 *SRL1* regulation mechanism in leaf development due to the limit of the sampling location and the
89 limit of the technology for gene expression profiling (microarray). While the previous proteomic
90 study was with *clld1*, which exhibited extra defects in addition to adaxially rolled leaves. Part of
91 the differentially expressed proteins obtaining from this study may not relate to the leaf
92 development but the other developmental processes due to the multiple defects in *clld1*. To obtain
93 a more complete view of the *SRL1* regulation mechanism in leaf development, we created a *SRL1*
94 knockout mutant by CRISPR/Cas9, and compared the gene expression profiles of the mature
95 leaves between the knockout mutant and its control.

96 **Results**

97 **Generation of *SRL1* KO lines by CRISPR/Cas9**

98 In order to study the biological function of *SRL1*, we created *SRL1* knockout (KO) lines by
99 CRISPR/Cas9, with the target site located in the first exon (Fig. 1a). We obtained 14 T₀ transgenic

100 plants. For each T₀ transgenic plants, the target sequence was identified by Sanger-sequencing of
101 the target-containing amplicons followed by decoding via DsDecodeM (Liu et al 2015). Half of
102 the T₀ transgenic plants (7 of 14) were identified as non-KO plants, in which contained the intact
103 *SRL1* and showed no defects in leaf development; the other 7 plants were identified as knock out
104 mutants with 1 bp insertion (T or C) in the first exon resulting in a frame shift with premature
105 transcription termination (Additional file 1: Table S1, Fig. 1b~c). All the knockout mutants
106 exhibited adaxially rolled leaf which were similar to that of the *srl1-1* and *srl1-2* (Xiang et al
107 2012) indicating that we had successfully created the *SRL1* knockout line (*srl1-KO*) as well as the
108 control line (non-KO), which could be available for the further transcriptomic study (Fig. 1d~f).

109 **Transcriptomic analysis**

110 To understand the gene regulatory network that controlled by *SRL1*, we analyzed the
111 transcriptomic data that generated from the mature leaves (60 days after germination) of the *SRL1*
112 knockout mutants *srl1-KO* and the control non-KO. We carried out the RNA-seq with three
113 biological replicates of *srl1-KO* and non-KO respectively. After filtering out the unqualified reads
114 from the raw data, we obtained 62.85, 56.16 and 56.06 million clean reads for the three KO
115 libraries and 55.25, 58.70 and 58.91 million clean reads for the three non-KO libraries. For each of
116 the six libraries, at least 94.02% of the clean reads had a quality score of Q30. The GC content
117 was 54.45%, 54.63% and 54.54% for KO libraries and 55.04%, 54.55% and 54.44% for non-KO
118 libraries. Using HISAT2 software (Kim et al 2015), more than 89.71% of clean reads were
119 successfully and uniquely mapped to the rice genome (Table 1). Furthermore, we evaluated the
120 correlation between the samples by Pearson's correlation coefficient using deepTool2 (Ramirez et

121 al 2016). The correlation was higher for the samples within group than that from different groups.
122 Taken together, all these results indicated the good quality of our sequencing data suggesting the
123 high confidence for the subsequence transcriptomic analysis results (Fig. 2a).

124 We detected 32,668 genes expression by RNA-seq at least in one set of the samples (Additional
125 file 2: Table S2), A total number of 3,178 genes were identified as differentially expressed genes
126 (DEGs) with the cutoff for FDR (False Discovery Rate) < 0.01 and absolute log₂FC (Fold
127 Change) > 1. Of these DEGs, 1,216 genes were significantly up regulated in the *srl1*-KO line,
128 while 1,962 genes were down regulated (Fig. 2b, Additional file 3: Table S3). Among these DEGs,
129 678 genes were annotated by KEGG (Kyoto Encyclopedia of Genes and Genomes) (Additional
130 file 4: Table S4). Three hundred seventy eight of 678 DEGs were assigned to 101 KEGG
131 pathways (Additional file 5: Table S5). Plant hormone signal transduction, plant-pathogen
132 interaction and starch & sucrose metabolism were the top three largest groups of DEGs according
133 to the KEGG pathways analysis (Fig. 2c). To further validate the RNA-seq data, the expression
134 quantification of 12 known leaf rolling related genes were determined by quantitative reverse
135 transcription polymerase chain reaction (qRT-PCR) including *OsZHD1*, *LC2*, *RL14*, *ACLI*,
136 *OsLBD3-7*, *YABI*, *NAL7*, *CFL1*, *ADLI*, *OsAGO1c*, *OsAGO1d* and *NRL2*. The selected genes
137 expression pattern determined by qRT-PCR were largely identical to those determined by
138 RNA-seq, which further indicated the credibility of the transcriptomic data (Fig. 2d).

139 **The expression profiles of leaf-rolling related genes**

140 To better understand the molecular regulatory mechanism of *SRL1* on controlling the leaf rolling,
141 we focused on the genes that previously known to relate to leaf rolling (Table 2). In our

142 transcriptomic study, many genes have been demonstrated to regulate leaf rolling by affecting
143 cytological architecture of leaf cells such as bulliform cells or the cuticle of leaves. Four genes
144 involved in the regulation of bulliform cells differentially expressed between the *srll*-KO and its
145 non-KO control. *OsZHD1* (FDR = 0.005, log₂FC = -1.402) and *OsLBD3-7* (FDR = 0.009, log₂FC
146 = -1.158) were significantly down regulated, while *RFS* (FDR = 0.003, log₂FC = 1.516) was
147 significantly up regulated. Moreover, *ACLI* (FDR = 0.011, log₂FC = -1.558) was up regulated.
148 These results were consistent with the fact that *SRL1* regulates leaf rolling by affecting bulliform
149 cells. In addition, *CFL1* (FDR = 0.011, log₂FC = -1.594), a gene related to leave cuticle
150 development was down regulated, indicating that the defects in the cuticle development may take
151 part responsibility for the leaf rolling in the *srll*-KO mutant.

152 In addition to the above genes, we checked the expression pattern of the leaf polarity related,
153 sclerenchymatous cells related and miRNA related genes, which have also been demonstrated to
154 play important roles in leaf rolling. However, we did not detect the significant expression change
155 for these genes in our transcriptomic data, indicating that *SRL1* may not regulate these kinds of
156 genes (Table 2).

157 In the previous *SRL1* study, it was suggested that genes encoding vacuolar H⁺-ATPases and
158 H⁺-pyrophosphatases might play important roles in regulating the formation of bulliform cells.
159 The microarray analysis revealed that ten vacuolar-related genes (*LOC_Os01g13130*,
160 *LOC_Os01g42430*, *LOC_Os01g55260*, *LOC_Os01g59800*, *LOC_Os02g07870*,
161 *LOC_Os02g24134*, *LOC_Os03g15650*, *LOC_Os03g58700*, *LOC_Os04g52190* and
162 *LOC_Os04g55040*) were up-regulated in *srll-1* mutant (Xiang et al 2012). In our study,

163 *LOC_Os04g52190/Os04g0611400* (FDR = 2.55×10^{-4} , $\log_2FC = 1.616$) was significantly up
164 regulated. Beside that, the other nine genes showed no significant change in our transcriptomic
165 study (Table 3).

166 In the previous *CLD1* study (Li et al 2017), a couple of genes related to secondary cell wall
167 cellulose were significantly down regulated ($FC > 2$) including a set of cellulose synthase gene
168 (*OsCESA1*, *OsCESA2*, *OsCESA3*, *OsCSLD4/NRL1*) (Hu et al 2010, Li et al 2009, Luan et al 2011,
169 Wang et al 2010) and a secondary cell wall-associate transcription factor (*SND1*) (Zhong et al
170 2006). In our study, *SND1* (FDR = 0.015, $\log_2FC = -1.753$) was down regulated. We did not detect
171 obvious change for *OsCESA1*, *OsCESA2*, *OsCESA3* and *OsCSLD4/NRL1*, however, the other two
172 cellulose synthase genes *OsCESA5* (FDR = 2.09×10^{-119} , $\log_2FC = -4.168$) and *OsCESA6* (FDR =
173 8.67×10^{19} , $\log_2FC = -2.197$), which did not change in the *cld1* mutant, showed remarkable
174 changes in the *srll*-KO mutant (Table 4). This may due to the different genetic background
175 between the *srll*-KO (Nipponbare, *sativa* L. ssp. *japonica*) mutant and the *cld1* mutant (93-11, *O.*
176 *sativa* L. ssp. *indica*).

177 **Discussion**

178 It has been previously demonstrated that many genes regulated the leaf rolling by affecting
179 bulliform cells, which located in the ridges of the vascular bundle near midrib on the adaxial
180 epidermis of leaf with large, empty, colorless and bubble-shape. In our study, *OsZHD1*,
181 *OsLBD3-7*, *RFS* and *ACL1* were differentially expressed between the *srll*-KO and the non-KO.
182 These genes are all related to the development of bulliform cells. Overexpression of *OsZHD1*, a
183 zinc finger homodomain class transcription factor, leads to an increase of bulliform cells that

184 causes abaxial rolling of leaves (Xu et al 2014). *OsLBD3-7* and *ACLI* regulate leaf rolling by
185 affecting both number and area of bulliform cells. Overexpressing *OsLBD3-7* induces adaxially
186 rolled leaves (Li et al 2016), while overexpressing *ACLI* leads to abaxial rolling leaves (Li et al
187 2010). *RFS* has been characterized as a key gene affecting leaf rolling, chloroplast development
188 and reactive oxygen species scavenging. The *rfs-1* mutants shows defects in vascular bundle and
189 bulliform cells development (Cho et al 2018). In addition, *OsMYB103L*, a *R2R3MYB* transcription
190 factor targeting *CESA* genes that are involved in the regulation of cellulose synthesis.
191 Overexpression of *OsMYB103L* displays adaxially rolled leaves due to reduced size of bulliform
192 cells (Yang et al 2014, Ye et al 2015). Although *OsMYB103L* did not show expression change in
193 our study, *OsCESA5* and *OsCESA6*, the downstream targets of *OsMYB103L* showed significant
194 change between the *srll*-KO and the non-KO.

195 The plant cuticle, a chemically heterogeneous lipophilic layer, protects the plants from biotic and
196 abiotic stress. It has been previously reported that defective cuticle development is responsible for
197 the rolling of the leaves. *CFLI*, encoding a WW domain protein, regulates cuticle development by
198 modulating the function of *HDGI*, which encodes a class IV homeodomain transcription factor.
199 Overexpression of *CFLI* led to severely impaired cuticle development resulting in the phenotype
200 of curly leaves (Wu et al 2011). In our study, *CFLI* was down regulated in the *srll*-KO indicated
201 that *SRLI* may also regulate the cuticle development.

202 In plants, the protons was pumped into vacuolar lumen by the electrochemical H⁺ gradient which
203 was created by vacuolar H⁺-ATPases and H⁺-pyrophosphatases to maintain the cellular ionic and
204 metabolism homeostasis (Ratajczak 2000). *SRLI* may repress the expression of the genes

205 encoding vacuolar H⁺-ATPases and H⁺-pyrophosphatases to suppress the enlargement of vacuolar
206 and formation of bulliform cells. Ten vacuolar-related genes were up regulated in the *srll-1*
207 mutant by microarray analysis (Xiang et al 2012), however, in our RNA-seq study, only one gene
208 (*LOC_Os04g52190/Os04g0611400*) was significantly up regulated in the *srll-KO*. The difference
209 between the two transcriptomic analyses may due to the different regions of sampling. For the
210 microarray analysis, cells abutting the midrib at the adaxial surface of leaf blades (5 days after
211 germination) that will become epidermal cells in wild type and probably bulliform cells in *srll-1*
212 were isolated by laser microdissection and used for microarray analysis, respectively. In our
213 RNA-seq, the mature leaves (60 days after germination) of the *srll-KO* and the control non-KO
214 were collected and subsequently used for the RNA-seq analysis. The precise sampling region for
215 the microarray analysis may contribute to the more sensitive detection for the particular genes that
216 involved in bulliform cells formation. As a coin has two sides, the restrictive sampling region may
217 limit the detection of the leaf rolling-related genes that involved in the other developmental
218 processes, which may be detected by our RNA-seq analysis.

219 **Conclusions**

220 In summarize, we generated the *SRLI* knock out line by CRISPR/Cas9, then carried out the
221 RNA-seq for studying the regulatory network that controlled by *SRLI* in regulating the rice leaf
222 rolling. A total number of 3,178 genes were identified as DEGs with 1,216 up-regulated genes and
223 1,962 down-regulated genes. Further more, a group of known leaf rolling related genes which
224 involves in bulliform cell and cuticle development including *OsZHD1*, *OsLBD3-7*, *RFS*, *ACLI*,
225 *CFLI*, *SND1*, *OsCESA5* and *OsCESA6* were up or down regulated in the *srll-KO*, indicating that

226 *SRLI* may control leaf rolling by regulating a couple of genes that affecting cytological
227 architecture of leaf cells such as bulliforms and cuticle of leaves.

228 **Methods**

229 **Plant materials and growth conditions**

230 Rice (*Oryza sativa* L.) plants were grown in the greenhouse at 30°C for days and 25°C for night.
231 The genetic background of the the transgenic plants was Nipponbare.

232 **Vector construction**

233 To knock out *SRLI*: Target site was designed online (<http://cbi.hzau.edu.cn/crispr/>), the optimal
234 target site with low off-target score and high sgRNA score was selected. We prepared the
235 CRISPR/Cas9 binary constructs as described previously (Ma et al 2015).

236 **Sample collection and RNA extraction**

237 Mature leaves (60 days after germination) from a single plant were collected, total RNA was
238 extracted using a Plant RNA Purification Kit: RNeasy Plant Mini Kit (74904, QIAGEN, Germany)
239 following the manufacturer's instructions. RNA degradation and contamination were monitored
240 on 1% agarose gels.

241 **Library construction and Illumina sequencing**

242 Library construction and RNA-seq were performed at Beijing BioMarker Technologies (Beijing,
243 China) in accordance with the institute's protocols and briefly described here. RNA concentration

244 was measured using NanoDrop 2000 (Thermo). RNA integrity was assessed using the RNA Nano
245 6000 Assay Kit of the Agilent Bioanalyzer 2100 system (Agilent Technologies, CA, USA). A total
246 amount of 1 µg RNA per sample was used as input material for the RNA sample preparations.
247 Sequencing libraries were generated using NEBNext Ultra™ RNA Library Prep Kit for Illumina
248 (NEB, USA) following manufacturer's recommendations and index codes were added to attribute
249 sequences to each sample. Briefly, mRNA was purified from total RNA using poly-T
250 oligo-attached magnetic beads. Fragmentation was carried out using divalent cations under
251 elevated temperature in NEBNext First Strand Synthesis Reaction Buffer (5X). First strand cDNA
252 was synthesized using random hexamer primer and M-MuLV Reverse Transcriptase. Second
253 strand cDNA synthesis was subsequently performed using DNA Polymerase I and RNaseH.
254 Remaining overhangs were converted into blunt ends via exonuclease/polymerase activities. After
255 adenylation of 3' ends of DNA fragments, NEBNext Adaptor with hairpin loop structure were
256 ligated to prepare for hybridization. In order to select cDNA fragments of preferentially 240 bp in
257 length, the library fragments were purified with AMPure XP system (Beckman Coulter, Beverly,
258 USA). Then 3 µl USER Enzyme (NEB, USA) was used with size-selected, adaptor-ligated cDNA
259 at 37°C for 15 min followed by 5 min at 95°C before PCR. Then PCR was performed with
260 Phusion High-Fidelity DNA polymerase, Universal PCR primers and Index (X) Primer. At last,
261 PCR products were purified (AMPure XP system) and library quality was assessed on the Agilent
262 Bioanalyzer 2100 system. The clustering of the index-coded samples was performed on a cBot
263 Cluster Generation System using TruSeq PE Cluster Kit v4-cBot-HS (Illumina) according to the
264 manufacturer's instructions. After cluster generation, the library preparations were sequenced on
265 Illumina HiSeq Xten PE150 platform (paired end 150 bp) and paired-end reads were generated. All

266 the raw data have been submitted to the NCBI GEO database under accession number of
267 GSE144729.

268 **RNA-seq data analysis**

269 Raw data (raw reads) of fastq format were firstly processed through in-house perl scripts. In this
270 step, clean data (clean reads) were obtained by removing reads containing adapter, reads
271 containing ploy-N and low-quality reads from raw data. At the same time, Q20, Q30, GC-content
272 and sequence duplication level of the clean data were calculated. These clean reads were then
273 mapped to the reference genome sequence (Os-Nipponbare-Reference-IRGSP-1.0:
274 <http://rapdb.dna.affrc.go.jp/download/irgsp1.html>). Only reads with a perfect match or one
275 mismatch were further analyzed and annotated based on the reference genome. HISAT2 tools soft
276 were used to map with reference genome (Kim et al 2015). Differential expression analysis of two
277 groups (KO samples and Non-KO samples) was performed using the DESeq2 (Love et al 2014).
278 DESeq2 provide statistical routines for determining differential expression in digital gene
279 expression data using a model based on the negative binomial distribution. The resulting P values
280 were adjusted using the Benjamini and Hochberg's approach for controlling the false discovery
281 rate. Genes with FDR (false discovery rate) < 0.01 found by DESeq2 & absolute log₂FC (Fold
282 Change) > 1 were assigned as differentially expressed.

283 **KO (KEGG Ortholog) and KEGG pathway enrichment analysis**

284 KO analysis: Gene function was annotated based on the KEGG Ortholog database; KEGG
285 pathway enrichment analysis: KEGG pathway enrichment analysis (<http://www.genome.jp/kegg/>)

286 was performed to identify differentially expressed genes (DEGs). KOBAS (Mao et al 2005)
287 software was used to test the statistical enrichment of differential expression genes in KEGG
288 pathways ($E \leq 1e-5$).

289 **qRT-PCR**

290 First-strand cDNA was synthesized from 1 μ g total RNA using the PrimeScript™ RT reagent Kit
291 (with gDNA Eraser) (RR047A, Takara, Japan) according to the manufacturer's instructions.
292 qRT-PCR were carried out using the ChamQ™ SYBR® qPCR Master Mix (Q311-01, Vazyme,
293 China) on the LightCycler® 480II (Roche) according to the manufacturer's instructions. Rice
294 Ubiquitin (*Os03g0234200*) was used as internal reference and gene expression level was
295 normalized to the Ubiquitin expression level. The primers were showed in Additional file 6: Table
296 S6.

297 Additional file 1: Table S1. The target site sequence of the 14 T₀ transgenic plants

298 Additional file 2: Table S2. All genes expression profile

299 Additional file 3: Table S3. Differentially expressed genes

300 Additional file 4: Table S4. Genes assigned to KEGG

301 Additional file 5: Table S5. Genes assigned to KEGG pathway

302 Additional file 6: Table S6. Primers used for qPCR for this study

303

304 **References**

305

- 306 Chen Q, Xie Q, Gao J, Wang W, Sun B, et al. 2015. Characterization of Rolled and Erect Leaf 1 in
307 regulating leave morphology in rice. *Journal of Experimental Botany* 66: 6047-58
- 308 Cho SH, Lee CH, Gi E, Yim Y, Koh HJ, et al. 2018. The Rice Rolled Fine Striped (RFS) CHD3/Mi-2
309 Chromatin Remodeling Factor Epigenetically Regulates Genes Involved in Oxidative Stress
310 Responses During Leaf Development. *Front Plant Sci* 9: 364
- 311 Cho SH, Paek NC. 2016. Regulatory role of the OsWOX3A transcription factor in rice root
312 development. *Plant Signal Behav* 11: e1184807
- 313 Dai M, Zhao Y, Ma Q, Hu Y, Hedden P, et al. 2007. The rice YABBY1 gene is involved in the feedback
314 regulation of gibberellin metabolism. *Plant Physiol* 144: 121-33
- 315 Fang L, Zhao F, Cong Y, Sang X, Du Q, et al. 2012. Rolling-leaf14 is a 2OG-Fe (II) oxygenase family
316 protein that modulates rice leaf rolling by affecting secondary cell wall formation in leaves.
317 *Plant Biotechnology Journal* 10: 524-32
- 318 Fujino K, Matsuda Y, Ozawa K, Nishimura T, Koshiba T, et al. 2008. NARROW LEAF 7 controls leaf
319 shape mediated by auxin in rice. *Molecular Genetics and Genomics* 279: 499-507
- 320 Hibara K, Obara M, Hayashida E, Abe M, Ishimaru T, et al. 2009. The ADAXIALIZED LEAF1 gene
321 functions in leaf and embryonic pattern formation in rice. *Dev Biol* 334: 345-54
- 322 Hu J, Zhu L, Zeng D, Gao Z, Guo L, et al. 2010. Identification and characterization of NARROW AND
323 ROLLED LEAF 1, a novel gene regulating leaf morphology and plant architecture in rice.
324 *Plant Mol Biol* 73: 283-92
- 325 Huang J, Li Z, Zhao D. 2016. Deregulation of the OsmiR160 Target Gene OsARF18 Causes Growth
326 and Developmental Defects with an Alteration of Auxin Signaling in Rice. *Scientific Reports* 6
- 327 Khew C-Y, Teo C-J, Chan W-S, Wong H-L, Namasivayam P, Ho C-L. 2015. Brassinosteroid insensitive
328 1-associated kinase 1 (OsI-BAK1) is associated with grain filling and leaf development in rice.
329 *Journal of Plant Physiology* 182: 23-32
- 330 Kim D, Langmead B, Salzberg SL. 2015. HISAT: a fast spliced aligner with low memory requirements.
331 *Nat Methods* 12: 357-60
- 332 Li C, Zou X, Zhang C, Shao Q, Liu J, et al. 2016. OsLBD3-7 Overexpression Induced Adaxially
333 Rolled Leaves in Rice. *PLoS One* 11: e0156413
- 334 Li L, Shi Z-Y, Li L, Shen G-Z, Wang X-Q, et al. 2010. Overexpression of ACL1 (abaxially curled leaf
335 1) Increased Bulliform Cells and Induced Abaxial Curling of Leaf Blades in Rice. *Molecular*
336 *Plant* 3: 807-17
- 337 Li M, Xiong G, Li R, Cui J, Tang D, et al. 2009. Rice cellulose synthase-like D4 is essential for normal
338 cell-wall biosynthesis and plant growth. *Plant J* 60: 1055-69
- 339 Li WQ, Zhang MJ, Gan PF, Qiao L, Yang SQ, et al. 2017. CLD1/SRL1 modulates leaf rolling by
340 affecting cell wall formation, epidermis integrity and water homeostasis in rice. *Plant J* 92:
341 904-23
- 342 Liu B, Li P, Li X, Liu C, Cao S, et al. 2005. Loss of Function of OsDCL1 Affects MicroRNA
343 Accumulation and Causes Developmental Defects in Rice. *Plant Physiology* 139: 296-305
- 344 Liu W, Xie X, Ma X, Li J, Chen J, Liu YG. 2015. DSDecode: A Web-Based Tool for Decoding of
345 Sequencing Chromatograms for Genotyping of Targeted Mutations. *Mol Plant* 8: 1431-3

346 Liu X, Li M, Liu K, Tang D, Sun M, et al. 2016. Semi-Rolled Leaf2 modulates rice leaf rolling by
347 regulating abaxial side cell differentiation. *J Exp Bot* 67: 2139-50

348 Love MI, Huber W, Anders S. 2014. Moderated estimation of fold change and dispersion for RNA-seq
349 data with DESeq2. *Genome Biol* 15: 550

350 Luan W, Liu Y, Zhang F, Song Y, Wang Z, et al. 2011. OsCD1 encodes a putative member of the
351 cellulose synthase-like D sub-family and is essential for rice plant architecture and growth.
352 *Plant Biotechnol J* 9: 513-24

353 Ma X, Zhang Q, Zhu Q, Liu W, Chen Y, et al. 2015. A Robust CRISPR/Cas9 System for Convenient,
354 High-Efficiency Multiplex Genome Editing in Monocot and Dicot Plants. *Mol Plant* 8:
355 1274-84

356 Ma Y, Zhao Y, Shanguan X, Shi S, Zeng Y, et al. 2017. Overexpression of OsRRK1 Changes Leaf
357 Morphology and Defense to Insect in Rice. *Frontiers in Plant Science* 8

358 Mao X, Cai T, Olyarchuk JG, Wei L. 2005. Automated genome annotation and pathway identification
359 using the KEGG Orthology (KO) as a controlled vocabulary. *Bioinformatics* 21: 3787-93

360 Ramirez F, Ryan DP, Gruning B, Bhardwaj V, Kilpert F, et al. 2016. deepTools2: a next generation web
361 server for deep-sequencing data analysis. *Nucleic Acids Res* 44: W160-5

362 Ratajczak R. 2000. Structure, function and regulation of the plant vacuolar H(+)-translocating ATPase.
363 *Biochim Biophys Acta* 1465: 17-36

364 Shi Z, Wang J, Wan X, Shen G, Wang X, Zhang J. 2007. Over-expression of rice OsAGO7 gene
365 induces upward curling of the leaf blade that enhanced erect-leaf habit. *Planta* 226: 99-108

366 Walter A, Silk WK, Schurr U. 2009. Environmental effects on spatial and temporal patterns of leaf and
367 root growth. *Annu Rev Plant Biol* 60: 279-304

368 Wang L, Guo K, Li Y, Tu Y, Hu H, et al. 2010. Expression profiling and integrative analysis of the
369 CESA/CSL superfamily in rice. *BMC Plant Biol* 10: 282

370 Wu L, Zhang Q, Zhou H, Ni F, Wu X, Qi Y. 2009. Rice MicroRNA Effector Complexes and Targets.
371 *The Plant Cell* 21: 3421-35

372 Wu R, Li S, He S, Wassmann F, Yu C, et al. 2011. CFL1, a WW domain protein, regulates cuticle
373 development by modulating the function of HDG1, a class IV homeodomain transcription
374 factor, in rice and Arabidopsis. *Plant Cell* 23: 3392-411

375 Xiang J-J, Zhang G-H, Qian Q, Xue H-W. 2012. SEMI-ROLLED LEAF1 Encodes a Putative
376 Glycosylphosphatidylinositol-Anchored Protein and Modulates Rice Leaf Rolling by
377 Regulating the Formation of Bulliform Cells. *Plant Physiology* 159: 1488-500

378 Xu P, Ali A, Han B, Wu X. 2018. Current Advances in Molecular Basis and Mechanisms Regulating
379 Leaf Morphology in Rice. *Front Plant Sci* 9: 1528

380 Xu Y, Wang Y, Long Q, Huang J, Wang Y, et al. 2014. Overexpression of OsZHD1, a zinc finger
381 homeodomain class homeobox transcription factor, induces abaxially curled and drooping leaf
382 in rice. *Planta* 239: 803-16

383 Yang C, Li D, Liu X, Ji C, Hao L, et al. 2014. OsMYB103L, an R2R3-MYB transcription factor,
384 influences leaf rolling and mechanical strength in rice (*Oryza sativa*L.). *BMC Plant Biology*
385 14: 158

386 Yang S-Q, Li W-Q, Miao H, Gan P-F, Qiao L, et al. 2016. REL2, A Gene Encoding An Unknown
387 Function Protein which Contains DUF630 and DUF632 Domains Controls Leaf Rolling in
388 Rice. *Rice* 9

389 Ye Y, Liu B, Zhao M, Wu K, Cheng W, et al. 2015. CEF1/OsMYB103L is involved in GA-mediated

390 regulation of secondary wall biosynthesis in rice. *Plant Molecular Biology* 89: 385-401
391 Zhang GH, Xu Q, Zhu XD, Qian Q, Xue HW. 2009. SHALLOT-LIKE1 is a KANADI transcription
392 factor that modulates rice leaf rolling by regulating leaf abaxial cell development. *Plant Cell*
393 21: 719-35
394 Zhang JJ, Wu SY, Jiang L, Wang JL, Zhang X, et al. 2015. A detailed analysis of the leaf rolling mutant
395 sll2 reveals complex nature in regulation of bulliform cell development in rice (*Oryza sativa*
396 L.). *Plant Biol (Stuttg)* 17: 437-48
397 Zhao S, Zhao L, Liu F, Wu Y, Zhu Z, et al. 2016. NARROW AND ROLLED LEAF 2 regulates leaf
398 shape, male fertility, and seed size in rice. *Journal of Integrative Plant Biology* 58: 983-96
399 Zhao SQ, Hu J, Guo LB, Qian Q, Xue HW. 2010. Rice leaf inclination2, a VIN3-like protein, regulates
400 leaf angle through modulating cell division of the collar. *Cell Res* 20: 935-47
401 Zhong R, Demura T, Ye ZH. 2006. SND1, a NAC domain transcription factor, is a key regulator of
402 secondary wall synthesis in fibers of Arabidopsis. *Plant Cell* 18: 3158-70
403 Zou L-p, Sun X-h, Zhang Z-g, Liu P, Wu J-x, et al. 2011. Leaf Rolling Controlled by the
404 Homeodomain Leucine Zipper Class IV Gene Roc5 in Rice. *Plant Physiology* 156: 1589-602

405

406 **List of Abbreviation**

407 DEGs: Differentially Expressed Genes

408 FC: Fold Change

409 FDR: False Discovery Rate

410 KO: Knock Out

411 qRT-PCR: quantitative Reverse Transcription Polymerase Chain Reaction

412 **Declarations**

413 **Ethics approval and consent to participate**

414 Not applicable

415 **Consent for publication**

416 Not applicable

417 **Availability of data and materials**

418 All data generated or analyzed during this study are included in this published article and its
419 additional files.

420 **Competing interests**

421 The authors have declared that no competing financial interests.

422 **Funding**

423 This research was supported by National Natural Science Foundation of China (Grant No.
424 31560381). the Project of High Level Innovation Team and Outstanding Scholar in Guangxi
425 Colleges and Universities (Third batch, 2016) and the Project of Scientific Research in Guangxi
426 Colleges and Universities (KY2015ZD004).

427 **Authors' contributions**

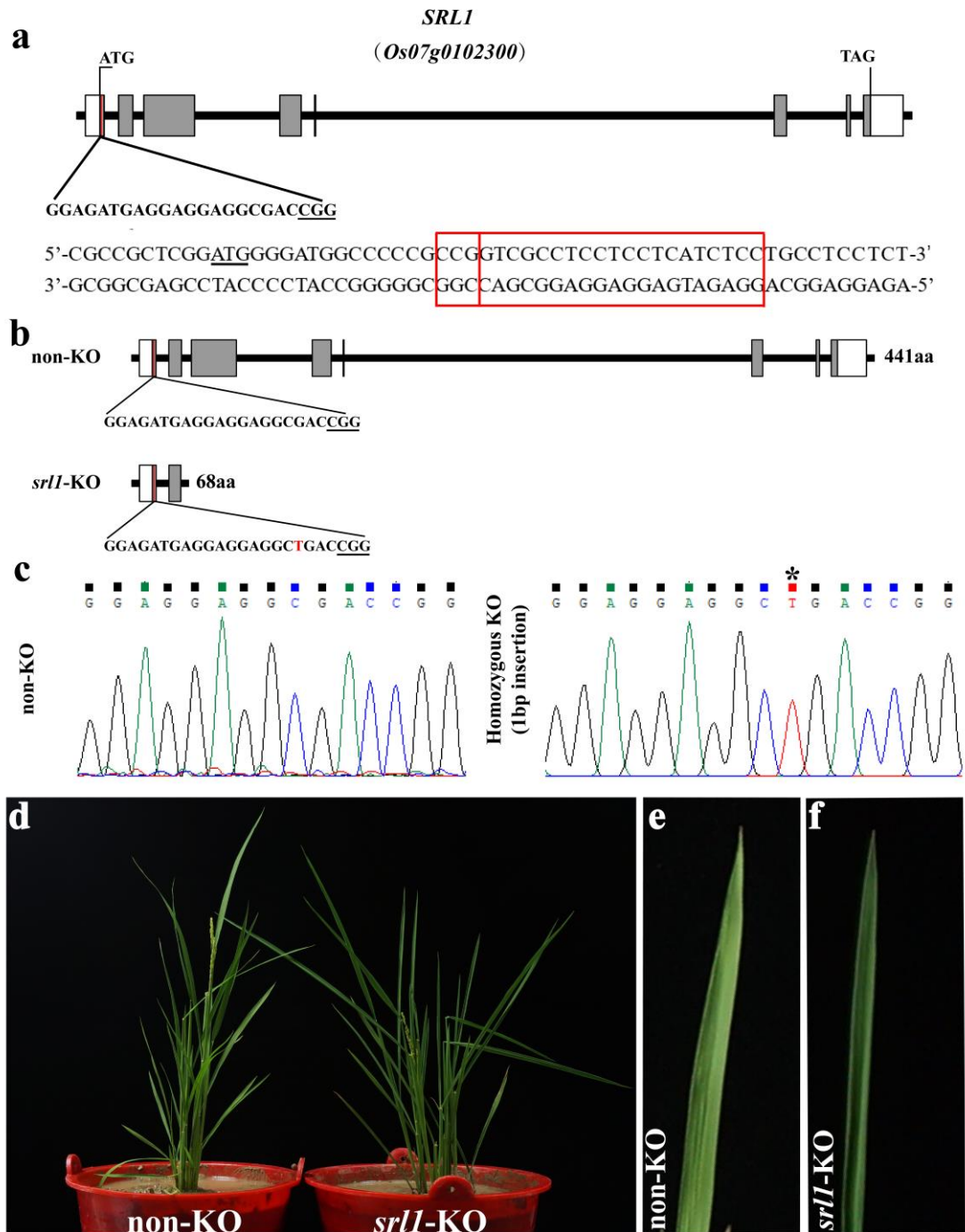
428 J.J. and J.W. planned and designed the research. X.L., M.L., B.Z., J.B., L.Z. and P.X. performed
429 experiments. J.J. wrote the manuscript. All authors read and approved the final manuscript.

430 **Acknowledgements**

431 Not applicable

432

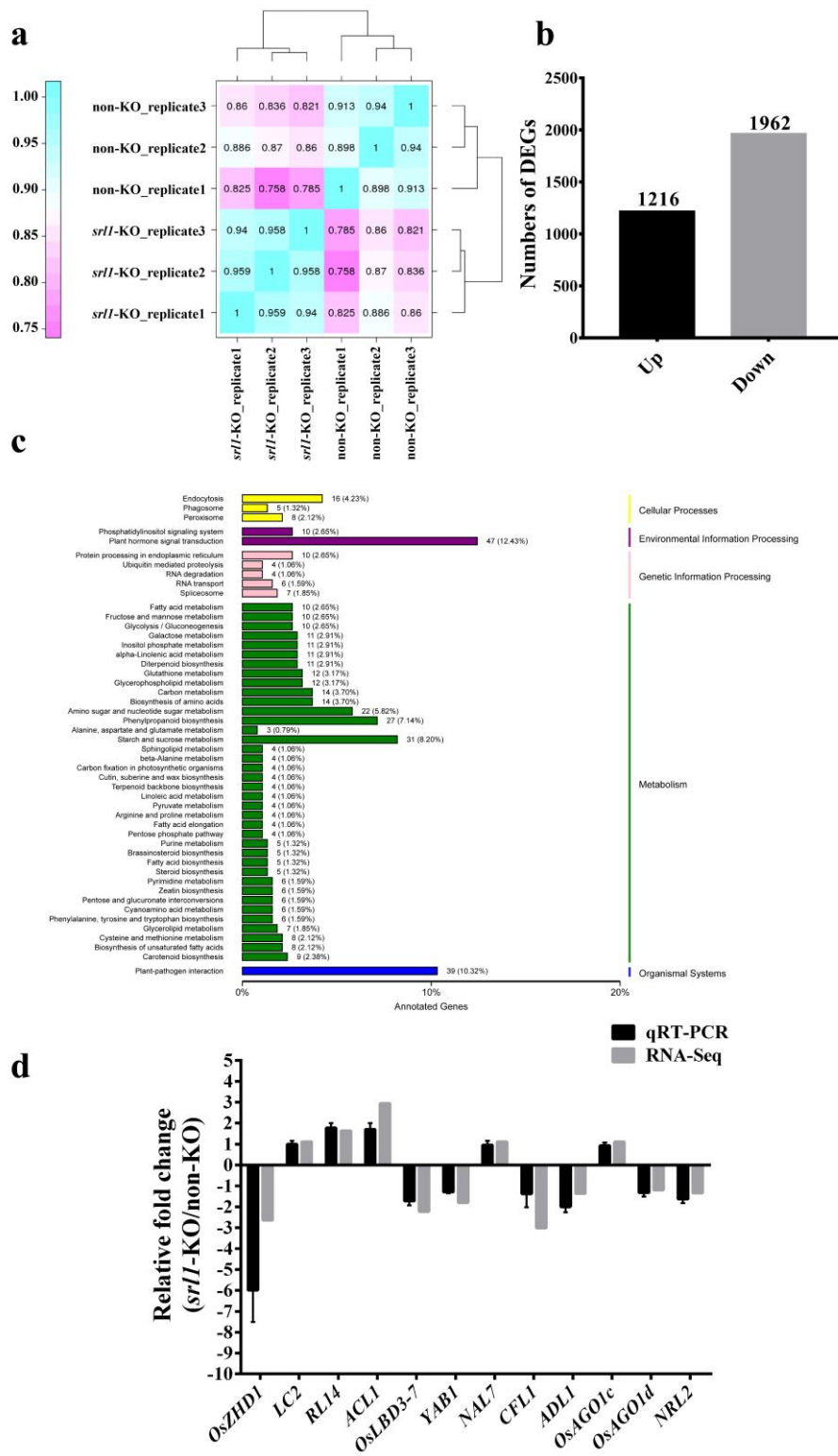
433



434

435 **Figure 1. The CRISPR/Cas9 target site of *SRL1* and phenotype of the KO plants**

436 (a) Schematic of *SRL1* gene structure and the CRISPR/Cas9 target site. The exon was indicated by gray rectangles, the
 437 untranslated region was indicated by white rectangles. The translation initiation codon (ATG) and termination codon (TGA) are
 438 shown. The target site nucleotides are shown in capital letters, and the protospacer adjacent motif (PAM) site is underlined. (b)
 439 Genomic structures at the *SRL1* locus in KO and non-KO line. (c) The original sequencing chromatograms of the target site for
 440 *SRL1* in non-KO and homozygous KO line. The protospacer adjacent motif (PAM) site is underlined, the "T" marked with an
 441 asterisk was the inserted in the *srl1*-KO. (d) Whole plant of non-KO and *srl1*-KO (e, f) Leaf blade phenotype of non-KO and
 442 *srl1*-KO.



443

444 **Figure 2. Overview of the DEGs**

445 (a) Correlation between any two replicates was calculated by Pearson's Correlation Coefficient value. (b) Numbers of
 446 up-regulated and down-regulated DEGs. (c) KEGG pathway assignment of the assembled unigenes (top 50 pathways according
 447 to enrichment factor). The vertical axis represents the enriched KEGG pathways and the horizontal axis represents the number of
 448 unigenes in each pathway. (d) The expression profiles of twelve leaf rolling related genes were validated by qPCR. Values are
 449 shown as means \pm s.d. (n = 3)

Table1. Statistical analysis of transcriptomic sequencing data

| Sample | Total reads | Mapped reads | Mapped ratio | Uniq mapped reads | Uniq mapped ratio | GC content | % \geq Q30 |
|----------------------------|-------------|--------------|--------------|-------------------|-------------------|------------|--------------|
| <i>srII</i> -KO_replicate1 | 62,850,674 | 59,408,986 | 94.52% | 56,381,278 | 89.71%; | 54.45% | 94.20% |
| <i>srII</i> -KO_replicate2 | 56,155,420 | 53,346,014 | 95.00% | 51,863,636 | 92.36% | 54.63% | 94.02% |
| <i>srII</i> -KO_replicate3 | 56,057,300 | 53,255,734 | 95.00% | 51,919,302 | 92.62% | 54.54% | 94.19% |
| non-KO_replicate1 | 55,252,706 | 52,949,414 | 95.83% | 51,221,015 | 92.70% | 55.04% | 94.28% |
| non-KO_replicate2 | 58,704,322 | 56,170,576 | 95.68% | 54,691,345 | 93.16% | 54.55% | 94.50% |
| non-KO_replicate3 | 58,905,796 | 56,352,819 | 95.67% | 54,756,848 | 92.96% | 54.44% | 94.49% |

451 Total reads: number of clean reads (single end); Mapped reads: number of clean reads which could be mapped to the reference genome;
 452 Mapped ratio: the percentage of the mapped reads; Uniq mapped reads: number of mapped reads which could uniquely be mapped to the
 453 reference genome; Uniq mapped ratio: the percentage of the uniq mapped reads; GC content: the content of G and C base in the clean
 454 reads. % \geq Q30: the percentage of clean reads whose the quality score were not less than 99.9%.

455

456

457

458

459

460

461

462

463

464

465

466

467

468

469

470

471

472

473

474

475

476

477

478

479

480

481

482

483

Table 2. The expression change of leaf rolling related genes in *srl1*-KO

| Gene function | Gene symbol | Gene ID (rap-db) | FDR | log ₂ FC |
|--------------------------------------|---------------------|---------------------|-------------|---------------------|
| Leaf Polarity (Adaxial Abaxial) | <i>ADL1</i> | <i>Os02g0709400</i> | 0.015505392 | -0.44226 |
| | <i>SLL1</i> | <i>Os04g0432600</i> | 0.424450406 | -0.2106 |
| | <i>OsAGO7</i> | <i>Os03g0449200</i> | 0.971027564 | 0.061401 |
| Bulliform Cells (Number and Size) | <i>SRL1</i> | <i>Os07g0102300</i> | 0.010497713 | -0.74096 |
| | <i>RFS</i> | <i>Os07g0497100</i> | 0.002628479 | 1.515866 |
| | <i>OsHox32</i> | <i>Os03g0640800</i> | 0.542687657 | -0.22059 |
| | <i>YAB1</i> | <i>Os07g0160100</i> | 0.284669838 | -0.84637 |
| | <i>OsZHD1</i> | <i>Os09g0466400</i> | 0.00494603 | -1.40154 |
| | <i>OsZHD2</i> | <i>Os08g0479400</i> | 0.568782633 | -0.6904 |
| | <i>LC2</i> | <i>Os02g0152500</i> | 0.767437117 | 0.165023 |
| | <i>RL14</i> | <i>Os10g0558900</i> | 0.228677074 | 0.710937 |
| | <i>NRL1</i> | <i>Os12g0555600</i> | 0.92137239 | -0.14938 |
| | <i>OsMYB103L</i> | <i>Os08g0151300</i> | 0.672191693 | 0.689681 |
| | <i>ROC5</i> | <i>Os02g0674800</i> | 0.000274182 | -0.52318 |
| | <i>PFL</i> | <i>Os06g0553200</i> | 0.158981616 | -1.56833 |
| | <i>ACL1</i> | <i>Os04g0415000</i> | 0.01109317 | 1.557548 |
| | <i>ACL2</i> | <i>Os02g0536500</i> | 0.610385337 | 0.705774 |
| | <i>REL1</i> | <i>Os01g0863500</i> | ND | ND |
| | <i>REL2</i> | <i>Os10g0562700</i> | 0.524590455 | -0.52246 |
| | <i>OsLBD3-7</i> | <i>Os03g0790600</i> | 0.009481005 | -1.15808 |
| | <i>NAL7</i> | <i>Os03g0162000</i> | 0.647658033 | 0.153462 |
| | <i>NAL2</i> | <i>Os11g0102100</i> | ND | ND |
| | <i>NAL3</i> | <i>Os12g0101600</i> | ND | ND |
| <i>OsI-BAK1</i> | <i>Os03g0440900</i> | 0.470309835 | 0.237016 | |
| <i>OsARF18</i> | <i>Os06g0685700</i> | 0.460616962 | 0.201005 | |
| <i>SLL2</i> | <i>Os07g0574400</i> | 8.44236E-05 | -1.02348 | |
| <i>OsRRK1</i> | <i>Os06g0693200</i> | 0.88057517 | -0.19566 | |
| Sclerenchymatous Cells | <i>SLL1</i> | <i>Os09g0395300</i> | 0.990395328 | 0.02204 |
| | <i>NRL2/SRL2</i> | <i>Os03g0308200</i> | 0.0352642 | -0.42714 |
| | <i>RL14</i> | <i>Os10g0558900</i> | 0.228677074 | 0.710937 |
| Cuticle Development | <i>CFL1</i> | <i>Os02g0516400</i> | 0.010961277 | -1.59358 |
| | <i>OsMYB103L</i> | <i>Os08g0151300</i> | 0.672191693 | 0.689681 |
| miRNAs | <i>OsAGO7</i> | <i>Os03g0449200</i> | 0.971027564 | 0.061401 |
| | <i>OsAGO1a</i> | <i>Os02g0672200</i> | 0.312503448 | -0.30481 |
| | <i>OsAGO1b</i> | <i>Os04g0566500</i> | 0.825927752 | -0.08416 |
| | <i>OsAGO1c</i> | <i>Os02g0831600</i> | 0.533440632 | 0.157662 |
| | <i>OsAGO1d</i> | <i>Os06g0729300</i> | 0.340339116 | -0.26243 |
| | <i>OsARF18</i> | <i>Os06g0685700</i> | 0.460616962 | 0.201005 |
| | <i>OsHB4</i> | <i>Os03g0640800</i> | 0.542687657 | -0.22059 |
| | <i>DCL1</i> | <i>Os03g0121800</i> | 0.669179001 | -0.5769 |

ND: not detected in the RNA-seq

Table 3. The expression change of some vacuolar related genes in *srll*-KO

| Gene ID | Annotation | FDR | log ₂ FC |
|------------------------------------|--|----------|---------------------|
| <i>LOC_Os01g13130/Os01g0232100</i> | Tonoplast membrane integral protein ZmTIP4-3 | 0.149376 | -0.87623 |
| <i>LOC_Os01g42430/Os01g0610100</i> | Vacuolar ATP synthase 21-kD proteolipid subunit C | 0.347985 | 0.20785 |
| <i>LOC_Os01g55260/Os01g0757400</i> | SKD1 protein (Vacuolar sorting protein4b) | 0.681726 | -0.36565 |
| <i>LOC_Os01g59800/Os01g0813500</i> | Vacuolar protein sorting36 family protein | 0.95445 | 0.017811 |
| <i>LOC_Os02g07870/Os02g0175400</i> | Vacuolar proton-ATPase subunit A | 0.028012 | 0.643565 |
| <i>LOC_Os02g24134/Os02g0437800</i> | Vacuolar protein-sorting protein45 homolog (AtVPS45) | 0.158677 | 0.46179 |
| <i>LOC_Os03g15650/Os03g0262900</i> | Vacuolar sorting protein9 domain-containing protein | 1.02E-08 | -0.98033 |
| <i>LOC_Os03g58700/Os03g0801600</i> | Vacuolar protein sorting-associated protein35 family protein | 0.018231 | 0.416066 |
| <i>LOC_Os04g52190/Os04g0611400</i> | Vacuolar sorting receptor homolog | 0.000255 | 1.615591 |
| <i>LOC_Os04g55040/Os04g0643100</i> | Vacuolar ATP synthase subunit D (EC 3.6.3.14) | 0.682713 | 0.116245 |

These genes were up regulated in the *srll-1* mutant

Table 4. The expression change of the Secondary cell wall cellulose related genes in *srII*-KO

| Gene function | Gene symbol | Gene ID (rap-db) | FDR | log ₂ FC |
|---------------------|---------------------|---------------------|-----------|---------------------|
| | <i>OsCSLD1</i> | <i>Os10g0578200</i> | 0.6927607 | 0.599779 |
| | <i>OsCSLD2</i> | <i>Os06g0111800</i> | 0.0005026 | -0.88051 |
| | <i>OsCSLD3</i> | <i>Os08g0345500</i> | ND | ND |
| | <i>OsCSLD4/NRL1</i> | <i>Os12g0555600</i> | 0.9213724 | -0.14938 |
| | <i>OsCSLD5</i> | <i>Os06g0336500</i> | ND | ND |
| | <i>OsCESA1</i> | <i>Os05g0176100</i> | 9.30E-05 | -0.89603 |
| | <i>OsCESA2</i> | <i>Os03g0808100</i> | 3.54E-28 | -1.9736 |
| Secondary cell wall | <i>OsCESA3</i> | <i>Os07g0424400</i> | 0.2319069 | 0.35963 |
| cellulose related | <i>OsCESA4</i> | <i>Os01g0750300</i> | 0.2985569 | -0.78159 |
| | <i>OsCESA5</i> | <i>Os03g0837100</i> | 2.09E-119 | -4.16828 |
| | <i>OsCESA6</i> | <i>Os07g0252400</i> | 8.67E-19 | -2.19716 |
| | <i>OsCESA7</i> | <i>Os10g0467800</i> | 0.6748408 | -0.65668 |
| | <i>OsCESA8</i> | <i>Os07g0208500</i> | 0.7860391 | -0.15179 |
| | <i>OsLAC17</i> | <i>Os10g0346300</i> | 0.3431087 | 1.111629 |
| | <i>SND1</i> | <i>Os06g0131700</i> | 0.0014968 | -1.75336 |
| | <i>VND4</i> | <i>Os06g0104200</i> | 0.8699304 | -0.29791 |
| | <i>OsDRP2B</i> | <i>Os02g0738900</i> | 0.3850803 | 0.282578 |

ND: not detected in the RNA-seq

Figures

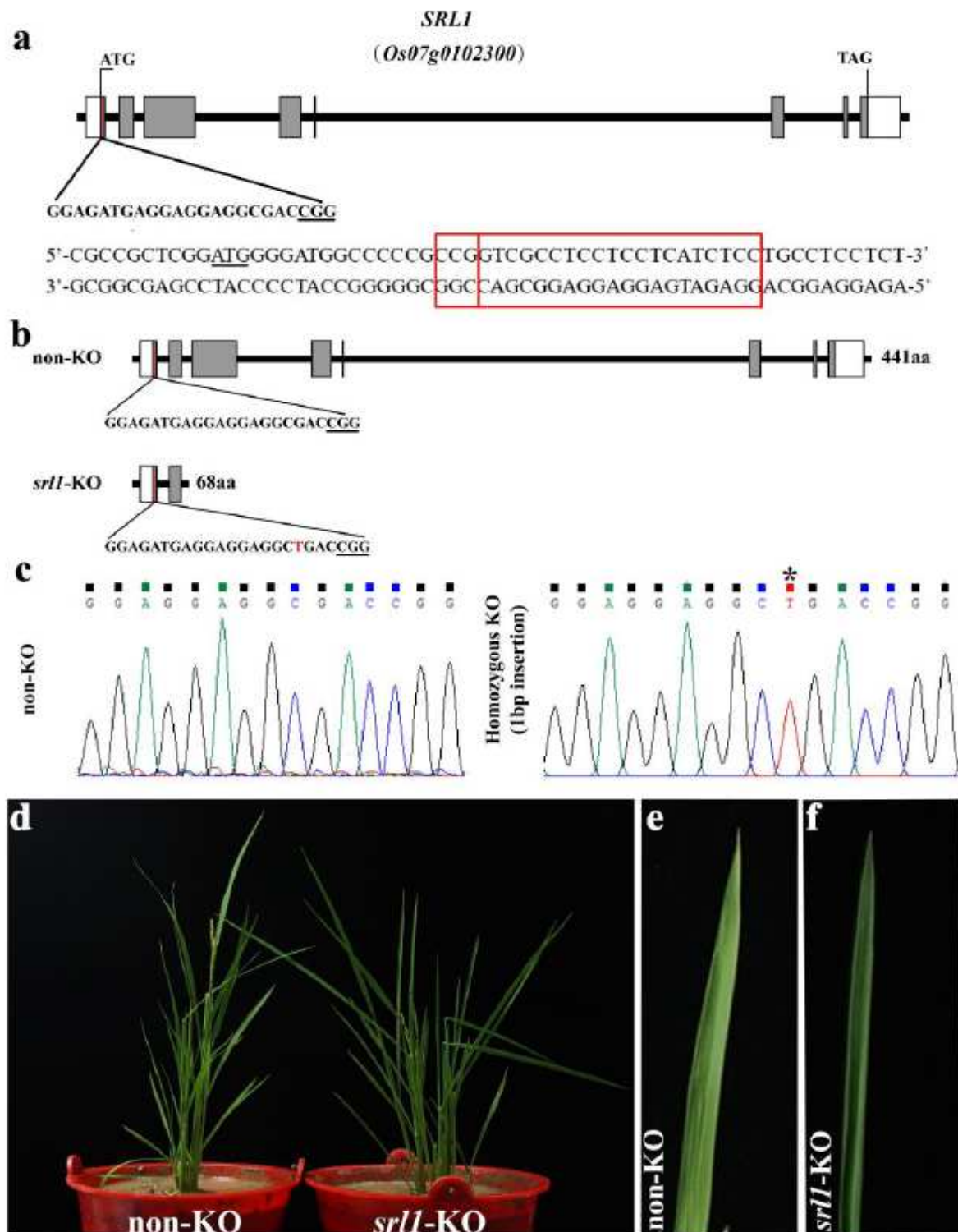


Figure 1

The CRISPR/Cas9 target site of *SRL1* and phenotype of the KO plants. (a) Schematic of *SRL1* gene structure and the CRISPR/Cas9 target site. The exon was indicated by gray rectangles, the untranslated region was indicated by white rectangles. The translation initiation codon (ATG) and termination codon

(TGA) are shown. The target site nucleotides are shown in capital letters, and the protospacer adjacent motif (PAM) site is underlined. (b) Genomic structures at the SRL1 locus in KO and non-KO line. (c) The original sequencing chromatograms of the target site for SRL1 in non-KO and homozygous KO line. The protospacer adjacent motif (PAM) site is underlined, the "T" marked with an asterisk was the inserted in the srl1-KO. (d) Whole plant of non-KO and srl1-KO (e, f) Leaf blade phenotype of non-KO and srl1-KO.

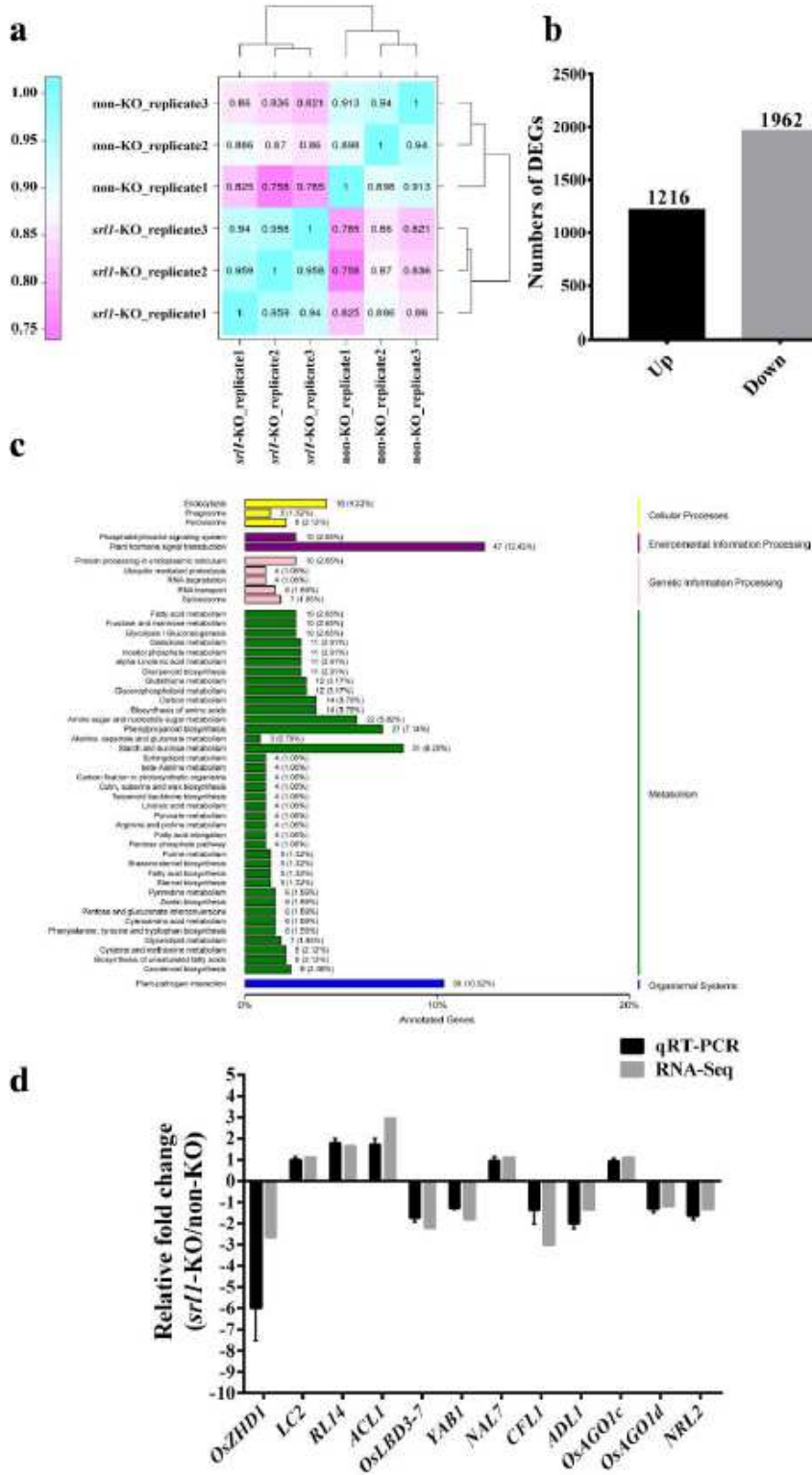


Figure 2

Overview of the DEGs. (a) Correlation between any two replicates was calculated by Pearson's Correlation Coefficient value. (b) Numbers of up-regulated and down-regulated DEGs. (c) KEGG pathway assignment of the assembled unigenes (top 50 pathways according to enrichment factor). The vertical axis represents the enriched KEGG pathways and the horizontal axis represents the number of unigenes in each pathway. (d) The expression profiles of twelve leaf rolling related genes were validated by qPCR. Values are shown as means \pm s.d. (n = 3)

Supplementary Files

This is a list of supplementary files associated with this preprint. Click to download.

- [TableS5.xlsx](#)
- [TableS3.xlsx](#)
- [TableS4.xlsx](#)
- [TableS1.docx](#)
- [TableS2.xlsx](#)
- [TableS6.docx](#)